

# Numerical detection of symmetry enriched topological phases with space group symmetry

Ling Wang,<sup>1,2</sup> Andrew Essin,<sup>1,2</sup> Michael Hermele,<sup>3</sup> and Olexei Motrunich<sup>2</sup>

<sup>1</sup>*Institute for Quantum Information and Matter,*

*California Institute of Technology, Pasadena, California 91125, USA*

<sup>2</sup>*Department of Physics, California Institute of Technology, Pasadena, California 91125, USA*

<sup>3</sup>*Department of Physics, 390 UCB, University of Colorado, Boulder CO 80309, USA*

(Dated: January 27, 2023)

Topologically ordered phases of matter, in particular so-called symmetry enriched topological (SET) phases, can exhibit quantum number fractionalization in the presence of global symmetry. In  $\mathbb{Z}_2$  topologically ordered states in two dimensions, fundamental translations  $T_x$  and  $T_y$  acting on anyons can either commute or anticommute. This property, crystal momentum fractionalization, can be seen in a periodicity of the excited-state spectrum in the Brillouin zone. We present a numerical method to detect the presence of this form of symmetry enrichment given a projected entangled pair state (PEPS); we study the minima of spectrum of correlation lengths of the transfer matrix for a cylinder. As a benchmark, we demonstrate our method using a modified toric code model with perturbation. An enhanced periodicity in momentum clearly reveals the anticommutation relation  $\{T_x, T_y\} = 0$  for the corresponding quasiparticles in the system.

PACS numbers: 05.30.Pr, 71.15.Qe, 75.10.Jm, 75.10.Kt

Topological order is the name given to a variety of long range entangled but gapped phases of matter, in particular to phases that support anyonic excitations with unusual braiding statistics. Unlike phases that fall within the Landau symmetry-breaking paradigm, topological order is defined without any reference to symmetry. However, it is still very interesting to ask what further phenomena emerge in systems with symmetry, either spontaneously broken or unbroken. The term “symmetry enriched topological” (SET) phases was proposed to describe phases that have the same topological order but are distinct in the presence of a symmetry [1–3].

In two dimensions the excitations in a topological phase are point-like anyons. When a symmetry is present, what are their quantum numbers? It turns out that these can be fractional; most prominently, anyons in quantum Hall states typically have fractional electric charge (the quantum number corresponding to a  $U(1)$  symmetry of the system) [4, 5]. The values of these quantum numbers are highly constrained, notably by the “fusion rules” of the topological theory; in the Laughlin quantum Hall state with filling fraction  $1/3$ , since three anyons give back an electron, the anyons must have charge  $e/3$ .

Can one distinguish SET phases given a wavefunction? For “internal” symmetries such as the  $U(1)$  mentioned above, one can use much the same method that has been proposed for measuring the fractional quantum numbers of end states in one-dimensional symmetry protected topological (SPT) phases using matrix product states (MPS) [6, 7]. In this Letter, we address this question for space group symmetries in the context of projected entangled pair states (PEPSs) [8].

$\mathbb{Z}_2$  topological phases with translation symmetry – We

are interested in the topological order familiar from  $\mathbb{Z}_2$  gauge theory,  $\mathbb{Z}_2$  spin liquids, and the toric code. There are two bosonic anyon species, often called  $e$  and  $m$ . Each sees the other with an Aharonov-Bohm phase of  $-1$  (they are mutual semions). When two-dimensional translation symmetry is present, the symmetry generators  $T_x$  and  $T_y$  may act nontrivially (projectively) on the anyons [2, 9]. A basis-independent characterization of these actions is given by the relations

$$\begin{aligned} T_x^e T_y^e T_x^{e-1} T_y^{e-1} &= \eta_e = \pm 1, \\ T_x^m T_y^m T_x^{m-1} T_y^{m-1} &= \eta_m = \pm 1, \end{aligned} \quad (1)$$

where  $T_x^e$  is the action of  $T_x$  on a single  $e$ , etc. When one of these relations evaluates to  $-1$  we say that translations act projectively, or that the anyon has fractional crystal momentum or a nontrivial fractionalization class, a notion closely related to Wen’s projective symmetry group [10].

One can interpret the nontrivial  $e$  relation as the presence of an  $m$  in each unit cell of the lattice, which the  $e$  sees as a background  $\pi$  magnetic flux. It is straightforward to show, based on this observation or directly from the relations above, that if  $e$  has fractional crystal momentum, the spectrum (and density of states) of two- $e$  scattering states is periodic under  $\mathbf{q} \rightarrow \mathbf{q} + (\pi, 0), (0, \pi), (\pi, \pi)$  [9, 11]. Assuming that  $e$  is the excitation of lowest energy, the low-energy edge of the continuum of excited states will reveal the fractionalization class of  $e$  in the dynamical structure factor of any operator that excites anyons. This is the main idea for detecting such SET states that we pursue in this paper.

*PEPS and transfer matrix* – PEPS is an ansatz that represents the wavefunction by locally entangled virtual pairs and a projector that map the virtual system to the

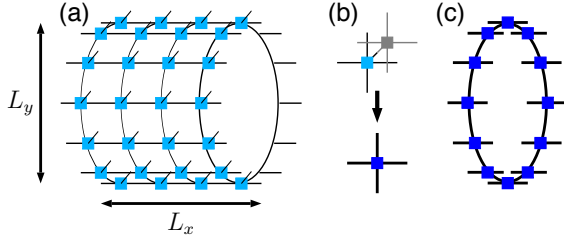


FIG. 1: (a) Schematic representation of a PEPS on a cylinder of size  $L_x \times L_y$ . (b) When multiplying bra and ket of PEPS, we sum over the physical degrees of freedom, group the virtual indices of a bond, and arrive at the double tensor of a single site. (c) Placing  $L_y$  double tensors on a ring and tracing out the virtual degrees on the shared bonds, we form the transfer matrix of the cylinder.

physical one [12]. It can capture a wide range of phases including many with topological order [13–20]. A one-dimensional version, the MPS [21], has been used to classify phases of symmetric, gapped spin systems based on the projective representation of the symmetry group [22–24]. Here, we propose a method based on PEPS for the spectra of correlation lengths (SCL) of the system, which allows us to distinguish SET phases described by simple PEPSs.

In one-dimensional gapped systems, properties of the ground state wave function (the MPS) are completely determined by the transfer matrix if translation symmetry is present. The spectrum of correlation lengths, which is given by the negative of the logarithm of (normalized) eigenvalues of the transfer matrix [21], is intuitively related to the spectrum of excitations made by all possible local operators [25].

The SCL can be generalized in two dimensions. For a cylindrical geometry (as in Fig. 1), we can similarly define SCL of the transfer matrix of a cylinder. If translation symmetry in the  $y$  direction is present, eigenvectors of the transfer matrix have well defined momentum quantum numbers  $k_y$ , and the minimum of the SCL is given by

$$\epsilon(k_x, k_y) = -\ln(|\lambda_{(k_x, k_y)}^{\max}|/\lambda_0), \quad (2)$$

where  $\lambda_{(k_x, k_y)}^{\max} = e^{ik_x} |\lambda_{(k_x, k_y)}^{\max}|$  is the leading eigenvalue of the transfer matrix with momentum  $k_y$  excluding ground states  $\lambda_0$ s (the largest eigenvalue among all sectors); in general it is a complex number with a phase  $e^{ik_x}$  where  $k_x$  is its momentum in the  $x$  direction [25]. We conjecture that  $\epsilon(k_x, k_y)$  at a given  $(k_x, k_y)$  are analogous to the low-energy edge of the two-anyon scattering continuum described earlier. Thus, we propose that the minima of the SCL can be used to distinguish SET phases, by analogy with the dynamic structure factor. The main goal of this Letter is to test this by examining the minima of the SCL of the transfer matrix.

*Modified toric code model* – To construct the simplest  $\mathbb{Z}_2$  spin liquid which realizes all possible projective quan-

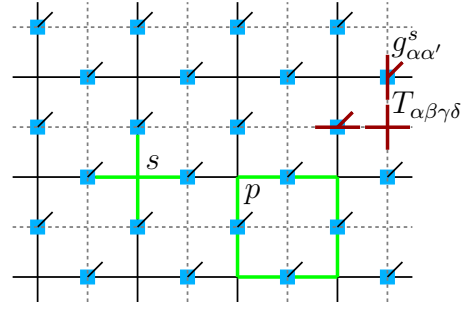


FIG. 2: A demonstration of the PEPS wavefunction of the toric code model in the  $\sigma^z$  basis. Green lines denote the star operator  $A_s$  and the plaquette operator  $B_p$ , and dark red lines denote the position of the 4-index  $T$  tensor and the 3-index  $g$  tensor, which are placed at the vertices and bonds of the dual lattice (denoted in dashed lines).

tum numbers of the translation symmetry, we consider the toric code Hamiltonian on a square lattice

$$H = -K_e \sum_s A_s - K_m \sum_p B_p, \quad (3)$$

where  $A_s = \prod_{l \in s} \sigma_l^x$  is defined on the vertex  $s$  and  $B_p = \prod_{l \in p} \sigma_l^z$  is defined on the plaquette  $p$ , and the sum runs over all vertices and all plaquettes. This Hamiltonian has four degenerate ground states [26]. Depending on the signs of  $K_m$  and  $K_e$ , the quasi-particles  $e$ ,  $m$ , if created, will move in a background of 0- or  $\pi$ -flux. That is,  $\eta_e = \text{sign} K_m$ ,  $\eta_m = \text{sign} K_e$  in Eq. (1). The ground states on a torus can be simply represented by PEPSs of bond dimension  $D = 2$ . We now describe the PEPSs for all choices of  $K_e = \pm 1$  and  $K_m = \pm 1$ .

The PEPSs are composed of 4-index tensors  $T_{\alpha\beta\gamma\delta}$  at the vertices and 3-index tensors  $g_{\alpha\alpha'}$  at the bonds of the direct (or dual) lattice, where  $s$  represents physical degrees of freedom and Greek letters represent virtual ones. Whether we take the direct or dual lattice depends on the choice of using a local  $\sigma^x$  or  $\sigma^z$  basis. Figure 2 represents a PEPS defined in the  $\sigma^z$  basis, where the tensor  $T_{\alpha\beta\gamma\delta}$  is placed at the vertices of the dual lattice; this is the representation we choose throughout this paper unless specified otherwise. The virtual index runs from 0 to 1, where 0 means  $|\uparrow\rangle$  and 1 means  $|\downarrow\rangle$ . The wave function has the form  $|\psi\rangle = \text{Tr}\{T^{\otimes V} g^{\otimes B}\}$ , where  $V$  means all vertices and  $B$  means all bonds, and the trace is taken over all common virtual degrees. The  $T$ -tensor is

$$T_{\alpha\beta\gamma\delta} = \begin{cases} 1, (0,0) & (\alpha + \beta + \gamma + \delta) \% 2 = 0 \\ 0, (1,1) & (\alpha + \beta + \gamma + \delta) \% 2 = 1 \end{cases}, \quad (4)$$

which, together with the condition that the only non-zero elements of the  $g$ -tensor are  $g_{ss}^s$  (see below), enforces the condition  $B_p|\psi\rangle = +(-)|\psi\rangle$ , corresponding to  $K_m > 0$

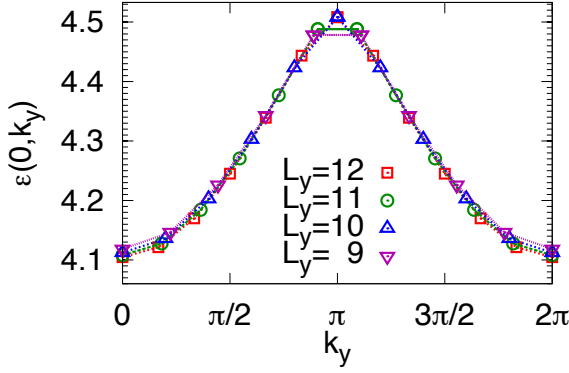


FIG. 3: The minima of SCL at momentum  $k_y$  for coupling  $K_m > 0$  and  $K_e > 0$  using PEPS at  $w = 0.9$ . Since all eigenvalues of the transfer matrix are real and positive, only  $\epsilon_{(0,k_y)}$  is presented.

( $K_m < 0$ ). The elements of the  $g$ -tensor are

$$g_{\alpha\alpha'}^s = \begin{cases} a, & \alpha = \alpha' = s = 0 \\ 1, & \alpha = \alpha' = s = 1 \\ 0, & \text{otherwise,} \end{cases} \quad (5)$$

where  $a$  is some number which can also depend on the position of the bond. We ask that the wave function satisfies  $A_s|\psi\rangle = +(-)|\psi\rangle$  for  $K_e > 0$  ( $K_e < 0$ ); this is nothing but asking that the amplitudes for configurations related by flipping the four spins on the vertex  $s$  differ by  $+$  ( $-$ ). If  $K_e > 0$  the solution is obvious:  $a = 1$  on all bonds. However, if  $K_e < 0$ , it requires one and only one  $a$  on each plaquette of the dual lattice to be  $-1$ , in which case one has to break the lattice translation symmetry in one direction in order to keep the bond dimension  $D = 2$  (see Appendix).

The excitations of the Hamiltonian Eq. (3) have no dynamics, which corresponds in the ground state  $|\psi\rangle$  to the fact that all spin configurations satisfying Eq. (4-5) have equal weight in magnitude. To create some dynamics without increasing the bond dimension of the tensor, we put a local diagonal operator  $\text{diag}(w, 1)$  on each physical spin with  $0 \leq w \leq 1$ , which corresponds to a ground state of the Hamiltonian [27, 28]

$$\begin{aligned} H' &= H + K_e \sum_s w^{-\sum_{l \in s} \sigma_l^z} \\ &\approx H + h \sum_l \sigma_l^z + \text{const.} \end{aligned} \quad (6)$$

Here, the Zeeman field  $h = -2K_e \log w$  is a good description of the perturbed state for  $h \ll K_e$ , or  $w \approx 1$ . Throughout this paper, we use  $w = 0.9$ , which corresponds to  $h \ll |K_m|, |K_e|$  and is deep in the topologically ordered phase. For the phase diagram of the modified PEPS as a function of  $w$  in case of  $K_m < 0$  and  $K_e > 0$ , see Appendix.

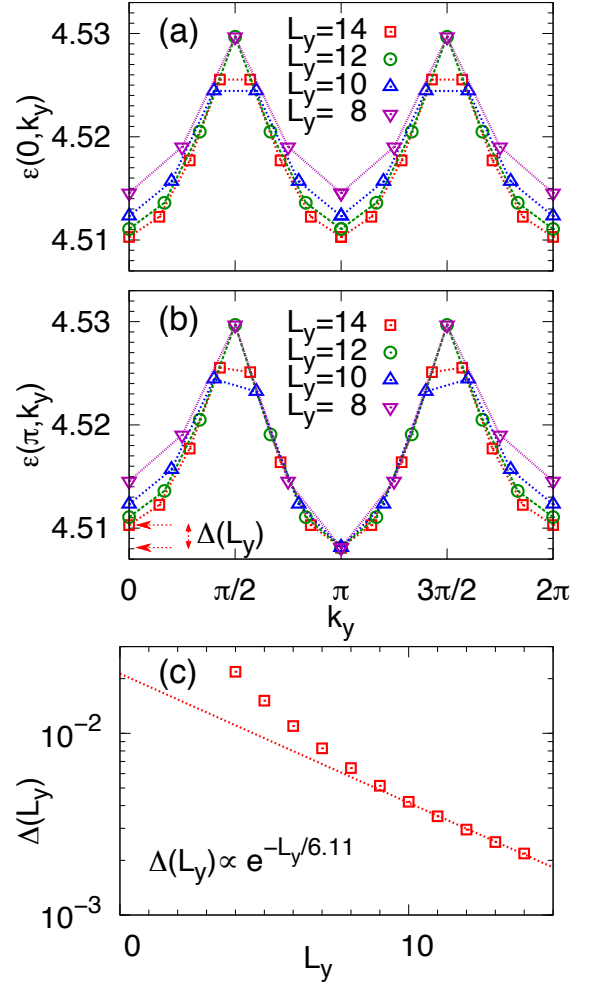


FIG. 4: The minima of SCL at momentum  $k_y$  for coupling  $K_m < 0$  and  $K_e > 0$  using PEPS at  $w = 0.9$  for even  $L_y$ . (a)  $\epsilon_{(0,k_y)}$  corresponds to the largest real and positive  $\lambda$  in sector  $k_y$  except  $\lambda_0$ s. (b)  $\epsilon_{(\pi,k_y)}$  corresponds to the smallest real and negative  $\lambda$  in sector  $k_y$ . (c) The splitting  $\Delta(L_y) = \epsilon_{(\pi,0)} - \epsilon_{(\pi,\pi)}$  as illustrated in (b) vanish exponentially as a function of length  $L_y$ .

*Numerical detection of the projective quantum number under translation symmetries* – We take the PEPS wave functions described above and calculate the SCL of the transfer matrix [see Fig. 1(b)] for different signs of  $K_m$  and  $K_e$ . The transfer matrix of a cylinder with translation symmetry  $T_y$  can be block-diagonalized in momentum basis, which means each left and right eigenvector has a well defined momentum quantum number  $k_y$ . We start by explicitly writing the transfer matrix in real space into a block diagonal form in momentum space (see Appendix). Once we have obtained the transfer matrix in momentum basis, we diagonalize each block with momentum  $k_y = 2\pi m/L_y, m = 0, 1, \dots, L_y - 1$ , find the minima of the normalized SCL  $\epsilon_{(k_x, k_y)} = -\ln(|\lambda_{(k_x, k_y)}^{\max}|/\lambda_0)$ , and plot  $\epsilon_{(k_x, k_y)}$  as a function of  $k_y$  for  $k_x = 0$  and  $\pi$ . Fig. 3 illustrates the minima of the SCL for  $K_m > 0$  and  $K_e > 0$ ,

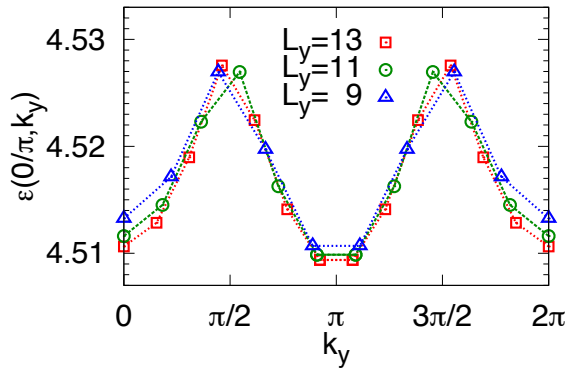


FIG. 5: The minima of SCL at momentum  $k_y$  for coupling  $K_m < 0$  and  $K_e > 0$  using PEPS at  $w = 0.9$  for odd length  $L_y$ . Since eigenvalues including the largest come in  $\pm$  pairs,  $\epsilon_{(0,k_y)}$  and  $\epsilon_{(\pi,k_y)}$  are identical.

in which case, all eigenvalues of the transfer matrix are real and positive. The results for  $K_m < 0$ ,  $K_e > 0$  and  $L_y$  even are presented in Fig. 4:  $\epsilon_{(0,k_y)}$  corresponds to the largest real and positive eigenvalue  $\lambda$  at each  $k_y$  excluding the two degenerate  $\lambda_0$ s at  $k_y = 0$ , while  $\epsilon_{(\pi,k_y)}$  corresponds to the smallest real and negative eigenvalue  $\lambda$  at each  $k_y$ . In the case of odd  $L_y$  for  $K_m < 0$  and  $K_e > 0$ , matrices at each  $k_y$  further form into two non-commuting blocks located on the upper-right and lower-left corner. This corresponds to a translation symmetry ( $T_x$ ) breaking case and all eigenvalues come in  $\pm$  pair, thus  $\epsilon_{(0/\pi,k_y)}$  are identical, as presented in Fig. 5. We find that the minima of the SCL are indeed doubly periodic when  $K_m < 0$ , but not when  $K_m > 0$ .

For the case of  $K_e < 0$  and  $K_m < 0$  ( $K_m > 0$ ), the resulting  $\epsilon_{(0,k_y)}$  are exactly the same as above, because the low-energy excitations are dictated by coupling  $K_m$  regardless of the sign of  $K_e$ . Note that when  $K_e < 0$ ,  $\epsilon_{(\pi,k_y)}$  is not accessible, because the transfer matrix at any  $L_y$  consists of adjacent two columns, thus all eigenvalues are positive.

If we want the projective quantum number of  $m$ -particles, we can take a perturbed Hamiltonian as

$$H'' = -K_e \sum_s A_s - K_m \sum_p B_p + h' \sum_l \sigma_l^x \quad (7)$$

instead, and correspondingly choose a PEPS representation defined in the  $\sigma^x$  basis, where acting with a local operator  $\text{diag}(w, 1)$  is equivalent to adding a perturbation  $\delta H = h' \sum_l \sigma_l^x$ . The low-energy excitations are two  $m$ -particles and the sign of  $K_e$  determines whether the  $m$ -particle hops in a background of 0- or  $\pi$ -flux on the dual lattice. Once the projective quantum numbers  $\eta_e$  and  $\eta_m$  are known, one completely determines SET class of the state if the symmetry group consists only of translation [2].

*Conclusion* – We have presented the first known numerical method to distinguish symmetry enriched topo-

logical (SET) phases with fractionalized translation symmetry. This method uses the spectrum of correlation lengths (SCL) of the transfer matrix on a cylinder to represent qualitatively the excitation spectrum of the system as a function of  $k_y$  for special  $k_x = 0, \pi$ , if the ground state wave function is available in terms of projected entangled pair state (PEPS). From the fact that the non-trivial fractional quantum numbers of quasi-particles under translation symmetries will be manifest as enhanced Brillouin zone periodicity in the dispersion relation, one can read out the projective quantum number of the low energy quasiparticles from the behavior of the minima of SCL. We bench-marked this method with the toric code model under perturbation. Modifying the sign of the coupling coefficients in front of operator  $A_s$  and  $B_p$  and the perturbation terms, we were able to generate topologically ordered ground states with preferred  $e$ -particle or  $m$ -particle low-energy excitations in a background of either 0 or  $\pi$  magnetic flux, which realizes all symmetry classes with this topological order and symmetry [2]. We expressed the ground states of the modified toric code Hamiltonians as bond-dimension  $D = 2$  PEPSs and calculated the minima of the SCL of the transfer matrix on a cylinder, and the pattern of SCL revealed the fractional quantum numbers of the low energy quasiparticles under translation symmetries.

This method can be generalized to detect projective quantum numbers of SET phases under a broader symmetry group including translations and other space group symmetries.

*Acknowledgment* – We would like to thank F. Verstraete and R. Mong for useful discussion. This work was supported by the Institute for Quantum Information and Matter, an NSF Physics Frontiers Center with support of the Gordon and Betty Moore Foundation through Grant GBMF1250, by the David and Lucile Packard foundation (M.H.), and by the National Science Foundation through grant DMR-1206096 (O.M.).

- 
- [1] L.-Y. Hung and X.-G. Wen, Quantized topological terms in weak-coupling gauge theories with a global symmetry and their connection to symmetry-enriched topological phases, Phys. Rev. B **87**, 165107 (2013).
  - [2] A. M. Essin and M. Hermele, Classifying fractionalization: Symmetry classification of gapped  $\mathbb{Z}_2$  spin liquids in two dimensions, Phys. Rev. B **87**, 104406 (2013).
  - [3] Y.-M. Lu and A. Vishwanath, Classification and Properties of Symmetry Enriched Topological Phases: A Chern-Simons approach with applications to  $\mathbb{Z}_2$  spin liquids, (2013), arXiv:1302.2634 (unpublished).
  - [4] D. C. Tsui, H. L. Stormer and A. C. Gossard, Two-Dimensional Magnetotransport in the Extreme Quantum Limit, Phys. Rev. Lett. **48**, 1559 (1982).
  - [5] R. B. Laughlin, Anomalous Quantum Hall Effect: An Incompressible Quantum Fluid with Fractionally Charged

- Excitations, Phys. Rev. Lett. **50**, 1395 (1983).
- [6] C. Y. Huang, X. Chen and F. Pollmann, Detection of symmetry-enriched topological phases, Phys. Rev. B **90**, 045142 (2014).
- [7] F. Pollmann and A. M. Turner, Detection of symmetry-protected topological phases in one dimension, Phys. Rev. B **86**, 125441 (2012).
- [8] F. Verstraete and J. I. Cirac, Renormalization algorithms for Quantum Many Body Systems in two and higher dimensions, (2004), arXiv:cond-mat/0407066 (unpublished).
- [9] A. Essin and M. Hermele, Spectroscopic signatures of crystal momentum fractionalization, (2014), arXiv:1401.1846 (unpublished).
- [10] X.-G. Wen, Quantum orders and symmetric spin liquids, Phys. Rev. B **65**, 165113 (2002).
- [11] X.-G. Wen, Quantum order: a quantum entanglement of many particles, Phys. Lett. A **300**, 175 (2002).
- [12] F. Verstraete, V. Murg and J. I. Cirac, Matrix product states, projected entangled pair states, and variational renormalization group methods for quantum spin systems, Adv. Phys. **57**, 143 (2008).
- [13] F. Verstraete, M. M. Wolf, D. Perez-Garcia and J. I. Cirac, Criticality, the Area Law, and the Computational Power of Projected Entangled Pair States, Phys. Rev. Lett. **96**, 220601 (2006).
- [14] Z. C. Gu, M. Levin and X. G. Wen, Tensor-entanglement renormalization group approach as a unified method for symmetry breaking and topological phase transitions, Phys. Rev. B **78**, 205116 (2008).
- [15] Z. C. Gu, M. Levin, B. Swingle and X. G. Wen, Tensor-product representations for string-net condensed states, Phys. Rev. B **79**, 085118 (2009).
- [16] O. Buerschaper, M. Aguado and G. Vidal, Explicit tensor network representation for the ground states of string-net models, Phys. Rev. B **79**, 085119 (2009).
- [17] J. I. Cirac, D. Poilblanc, N. Schuch and F. Verstraete, Entanglement spectrum and boundary theories with projected entangled-pair states, Phys. Rev. B **83**, 245134 (2011).
- [18] D. Poilblanc, N. Schuch, D. Pérez-García and J. I. Cirac, Topological and Entanglement Properties of Resonating Valence Bond wavefunctions, Phys. Rev. B **86**, 014404 (2012).
- [19] N. Schuch, D. Poilblanc, J. I. Cirac and D. Pérez-García, Resonating valence bond states in the PEPS formalism, Phys. Rev. B **86**, 115108 (2012).
- [20] N. Schuch, I. Cirac and D. Pérez-García, PEPS as ground states: Degeneracy and topology, Ann. Phys. **325**, 2153 (2010).
- [21] S. Östlund and S. Rommer, Thermodynamic Limit of Density Matrix Renormalization, Phys. Rev. Lett. **75**, 3537 (1995).
- [22] X. Chen, Z.-C. Gu and X.-G. Wen, Classification of gapped symmetric phases in one-dimensional spin systems, Phys. Rev. B **83**, 035107 (2011).
- [23] N. Schuch, D. Pérez-García and I. Cirac, Classifying quantum phases using matrix product states and projected entangled pair states, Phys. Rev. B **84**, 165139 (2011).
- [24] F. Pollmann, A. M. Turner, E. Berg and M. Oshikawa, Entanglement spectrum of a topological phase in one dimension, Phys. Rev. B **81**, 064439 (2010).

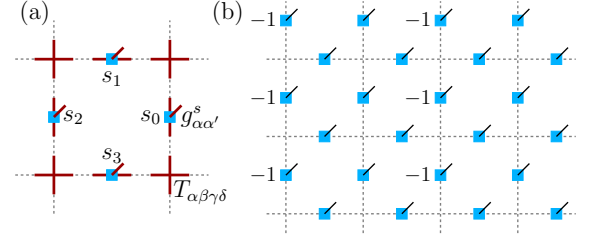


FIG. 6: (a) Demonstrate the vertices  $T_{\alpha\beta\gamma\delta}$  and bonds  $g_{\alpha\alpha'}^s$  affected by the operation of  $A_s$  on one plaquette of the dual lattice. (b) To meet the condition  $A_s|\psi\rangle = -|\psi\rangle$ , we choose  $a = -1$  on the vertical bonds of every other column of the dual lattice (as marked by  $-1$ ) and  $a = 1$  for all other bonds (without mark).

- [25] V. Zauner, D. Draxler, L. Vanderstraeten, M. Degroote, J. Haegeman, M. M. Rams, V. Stojevic, N. Schuch and F. Verstraete, Transfer Matrices and Excitations with Matrix Product States, (2014), arXiv:1408.5140 (unpublished).
- [26] A. Kitaev, Fault-tolerant quantum computation by anyons, Ann. Phys. **303**, 2 (2003).
- [27] C. Castelnovo and C. Chamon, Quantum topological phase transition at the microscopic level, Phys. Rev. B **77**, 054433 (2008).
- [28] N. Schuch, D. Poilblanc, J. I. Cirac and D. Pérez-García, Topological Order in the Projected Entangled-Pair States Formalism: Transfer Operator and Boundary Hamiltonians, Phys. Rev. Lett. **111**, 090501 (2013).

## APPENDIX

### PEPS for the ground state of toric code model with $K_e < 0$

In this section, we will discuss how to write a PEPS ground state for the toric code model with  $K_e < 0$  while keeping the bond dimension  $D = 2$ .

We want to write the PEPS in the  $\sigma_z$  basis since our perturbation  $h \sum_l \sigma_l^z$  is simple in this basis. The PEPS is composed of a 4-index tensor  $T_{\alpha\beta\gamma\delta}$  of bond dimension  $D = 2$

$$T_{\alpha\beta\gamma\delta} = \begin{cases} 1, (0, ) & (\alpha + \beta + \gamma + \delta) \% 2 = 0 \\ 0, (1, ) & (\alpha + \beta + \gamma + \delta) \% 2 = 1, \end{cases} \quad (8)$$

for  $K_m > 0$  ( $K_m < 0$ ), and a 3-index tensor  $g_{\alpha\alpha'}^s$

$$g_{\alpha\alpha'}^s = \begin{cases} a, & \alpha = \alpha' = s = 0 \\ 1, & \alpha = \alpha' = s = 1 \\ 0, & \text{otherwise.} \end{cases} \quad (9)$$

Here  $a$  is a number and can be different at different positions in order to satisfy the following condition when  $K_e < 0$

$$A_s|\psi\rangle = -|\psi\rangle. \quad (10)$$



The action of  $A_s$  is to flip four spins on the plaquette of the dual lattice as in Fig. 6(a). Assuming that each  $g$ -tensor at four positions  $s_0, s_1, s_2, s_3$  in Fig. 6(a) shares the same constant  $a$ , then Eq. (10) means that  $a^{4-2n} = -1$  for  $n = 0, 1, \dots, 4$ , where  $n$  is the number of down spins in that plaquette. However, there is no solution for the set of equations  $a^0 = a^{\pm 2} = a^{\pm 4} = -1$ . In conclusion, one has to break the translation symmetry and let  $a$  be different at different positions in one plaquette. We can choose a pattern as in Fig. 6(b) to satisfy Eq. (10) for every  $s$ . This choice maintains the translation invariance in the  $y$  direction but doubles the unit cell in the  $x$  direction; in such a case the transfer matrix consists of two adjacent columns instead of just one. We find that the minima of the SCL  $\epsilon_{(0,k_y)}$  for  $K_e < 0$  are identical with those for  $K_e > 0$  if  $K_m$  is kept the same. This is expected since, in our system governed by Hamiltonian Eq. (6) in the main text, it is the  $e$ -particles that appear as low energy excitations and their dispersion is determined by the sign of  $K_m$  only (while the  $m$ -particles that are sensitive to the sign of  $K_e$  are still completely localized).

#### Phase diagram of the PEPS wavefunction by tuning parameter $w$ for $K_m < 0$ and $K_e > 0$

This section studies the phase diagram of the PEPS wavefunction by tuning parameter  $w$  [in the local operator  $\text{diag}(w, 1)$ ] from 1 to 0 for  $K_m < 0$ ,  $K_e > 0$ . In one limit, when  $w \approx 1$ , the state is deep in the topologically ordered phase. In the opposite limit,  $w \rightarrow 0$ , all spins tend to point down, but the constraint Eq. 8 requires that each plaquette has an odd number of up spins. These conditions together lead to a state where all configurations with one spin up in each plaquette contribute equally.

When  $w$  is in between 0 and 1, one can imagine that the entropy contributed from the massive number of configurations that meet Eq. 8 is competing with the Zeeman energy, and a valence bond solid order could emerge. As one varies  $w$  from 1 to 0, the PEPS wavefunction could go through a phase transition from the topologically ordered phase to a valence bond solid phase. Inside the valence bond solid phase, translation symmetry is spontaneously broken in the thermodynamic limit, but at any finite size, the ground states are degenerate. We expect that two degenerate eigenvalues with  $\pm 1$  will appear as the leading eigenvalues of the transfer matrix; whereas in the topological phase, both leading eigenvalues are  $+1$ .

We now try to identify this phase transition using techniques discussed in the paper. We define  $\gamma_{(k_x, k_y)}$ , which roughly represents the gap to the ground state at momentum  $(k_x, k_y)$ , using eigenvalues of the transfer matrix:

$$\gamma_{(k_x, k_y)} = \begin{cases} -\ln(|\lambda_{(k_x, k_y)}^1|/\lambda_0), & k_x = k_y = 0 \\ -\ln(|\lambda_{(k_x, k_y)}^{\max}|/\lambda_0), & \text{otherwise} \end{cases}, \quad (11)$$

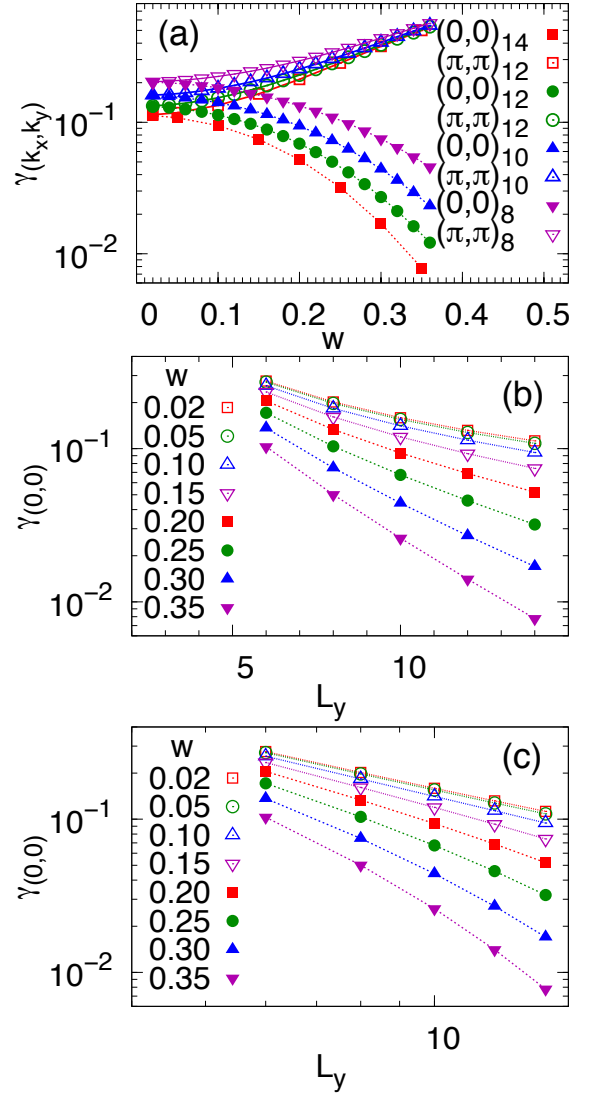


FIG. 7: (a) The ground state gap  $\gamma_{(k_x, k_y)}$  for coupling  $K_m < 0$   $K_e > 0$  as a function of  $w$  at special points  $(0, 0)$  and  $(\pi, \pi)$  for the cylinder perimeters  $L_y = 8, 10, 12, 14$ . For various fixed  $w$ ,  $\gamma_{(0,0)}$  is plotted against  $L_y$  in (b) a semi-log plot and (c) a log-log plot.

[in the sector  $(0, 0)$  we take the subleading eigenvalue  $\lambda_{(k_x, k_y)}^1$ , otherwise the leading eigenvalue  $\lambda_{(k_x, k_y)}^{\max}$ ].  $\gamma_{(k_x, k_y)}$  is different from  $\epsilon_{(k_x, k_y)}$  defined earlier in that the splitting of  $\lambda_0$ , doubly degenerate in the thermodynamic limit in the topological phase, is explicitly calibrated by  $\gamma_{(0,0)}$ . We plot  $\gamma_{(k_x, k_y)}$  at special points  $(0, 0)$  and  $(\pi, \pi)$  as a function of  $w$  for cylinder perimeters  $L_y = 8, 10, 12, 14$  in Fig. 7(a). Note that all other gaps lie well above these two within the plotted range. We do not see a crossing of  $\gamma_{(0,0)}$  and  $\gamma_{(\pi, \pi)}$  as we vary  $w$ . Instead, we find that they approach each other, with  $\gamma_{(\pi, \pi)}$  slightly larger than  $\gamma_{(0,0)}$  when  $w$  is close to 0. In order to examine finite size effects we plot  $\gamma_{(0,0)}$  as a function of  $L_y$  at various fixed  $w$ , in a semi-log plot [in Fig. 7(b)] and

a log-log plot [in Fig. 7(c)]. The results are inconclusive; we cannot identify any critical point where a topological phase turns into a valence bond solid phase due to very large correlation length and insufficient system  $L_y$  size available.

### Diagonalizing the transfer matrix of a cylinder in momentum basis

In the general case, the transfer matrix, denoted as  $\mathbb{E}$ , of a cylinder of circumference  $L_y$  can be thought of as a Hamiltonian for a system composed of local degrees of freedom with Hilbert space dimension  $D^2$  ( $D$  is the bond dimension of PEPS) where each degree of freedom is composed of two virtual degrees of freedom. These local degrees of freedom are arranged in a ring with  $L_y$  “sites”. Note that the transfer matrix is generally not hermitian. The matrix elements of the transfer matrix in real space can be computed by specifying a basis vector  $|a\rangle$  (which denotes compactly configuration of all  $L_y$  local degrees of freedom) and multiplying it by the transfer matrix

$$\mathbb{E}|a\rangle = \sum_b h_{ba}|b\rangle, \quad (12)$$

where  $h_{ba} = \langle b|\mathbb{E}|a\rangle$  is the matrix element.

The transfer matrix commutes with translations  $T$  in the  $y$  direction and hence can be diagonalized simultaneously with  $T$ . The eigenvalues of  $T$  have the form  $e^{ik}$  where  $k = 2\pi m/L_y$ ,  $m = 0, 1, \dots, L_y - 1$ . We construct the corresponding eigenspace  $V_k$  as follows.

First, we consider classes of real-space configurations that are related to each other by an action of  $T$ :  $|a\rangle$  and  $|a'\rangle$  belong to the same class if  $|a'\rangle = T^\ell|a\rangle$  for some  $\ell$ . It is easy to see that we can specify each class by one representative member  $|a\rangle$ , while all other members are given by  $T^\ell|a\rangle$ ,  $\ell = 0, 1, \dots, R_a - 1$ , where  $R_a$  is the smallest number such that  $T^{R_a}|a\rangle = |a\rangle$ ; the “periodicity”  $R_a$  must be less than or equal to  $L_y$  since  $T^{L_y} = 1$ . For a given momentum  $k$ , if  $kR_a$  is an integer multiple of  $2\pi$ , then out of the states in this class we can construct a single normalized eigenstate of  $T$  with eigenvalue  $e^{ik}$  as follows:

$$|a_k\rangle = \frac{1}{\sqrt{N_a}} \sum_{r=0}^{L_y-1} e^{-ikr} T^r |a\rangle, \quad (13)$$

where  $N_a$  is the normalization constant

$$N_a = L_y^2 / R_a. \quad (14)$$

On the other hand, if  $kR_a$  is not an integer multiple of  $2\pi$ , we cannot construct such an eigenstate from the states in this class; thus this class of configurations is not compatible with the momentum  $k$  and is not included as a basis state for  $V_k$ . By going over all classes that are compatible with  $k$ , we construct a complete basis of  $V_k$ , which we call the momentum basis.

We calculate the transfer matrix elements in the basis of  $V_k$  as follows

$$\begin{aligned} \mathbb{E}|a_k\rangle &= \frac{1}{\sqrt{N_a}} \sum_{r=0}^{L_y-1} e^{-ikr} T^r \mathbb{E}|a\rangle \\ &= \sum_{b'} h_{b'a} \frac{1}{\sqrt{N_a}} \sum_{r=0}^{L_y-1} e^{-ikr} T^r |b'\rangle, \end{aligned} \quad (15)$$

where  $|b'\rangle$  runs over all real-space basis states. Each such  $|b'\rangle$  belongs to some class whose representative we denote as  $|b\rangle$ , and hence there is  $l_{b'}$  such that

$$|b'\rangle = T^{-l_{b'}} |b\rangle. \quad (16)$$

Substituting this in Eq. (15), we have

$$\mathbb{E}|a_k\rangle = \sum_{b'} h_{b'a} e^{-ikl_{b'}} \frac{\sqrt{N_b}}{\sqrt{N_a}} |b_k\rangle, \quad (17)$$

where the summation runs over all real-space basis states  $|b'\rangle$  and not only the representative  $|b\rangle$ . Note that for each momentum-space basis state  $|b_k\rangle$ , the matrix element  $\langle a_k|\mathbb{E}|b_k\rangle$  obtains contributions from all  $b'$  that belong to the class which corresponds to  $|b_k\rangle$ .

After finding the matrix elements  $\langle b_k|\mathbb{E}|a_k\rangle$  in the basis in  $V_k$ , we can separately diagonalize the block diagonal transfer matrix for each momentum  $k$  and obtain the corresponding  $\epsilon_{k_y}$ .

In the present case, the transfer matrix actually simplifies since the structure of the  $T$  and  $g$  tensors are such that the labels  $\alpha\alpha'$  of the double tensor must coincide at each “site” in the transfer matrix;  $\alpha_i = \alpha'_i$  and  $\beta_i = \beta'_i$  ( $i = 0, 1, \dots, L_y - 1$ ), thus the size of Hilbert space is reduced from  $D^{2L_y}$  to  $D^{L_y}$ .